

Dynamic Analysis of a Structure Embedded
in an Elastic Stratum

by Hiroshi Tajimi

Abstract

This paper describes a theoretical and observatory study concerning soil-structure interaction. It is of great interest in the evaluation of

- (i) spring constant, effective mass and radiation damping related to the lateral resistance of surrounding soil, and
- (ii) input earthquake to structures through the side walls in contact with the subsoil.

The theoretical analysis was performed on a basis of the three-dimensional wave propagation theory in an elastic stratum overlying the rigid bed. When a cylindrical rigid body is embedded in the stratum of the depth H and undergoes rocking motion with the rotational angle $\phi e^{i\omega t}$, the reactive moment M_r due to the resistance of the stratum was obtained in the form

$$M_r = K_r \phi e^{i\omega t} = \frac{8\mu H^2 a}{\pi} \Gamma_1 (f_1 + if_2) \phi e^{i\omega t}$$

where a is the radius of cross section of the body, μ is the shear modulus of soil, and Γ_1 is dimensionless function of a/H and Poisson's ratio of soil. The complex function $f_1 + if_2$ gives dynamic effects and varies with ω/ω_g , h_g , a/H and Poisson's ratio of soil, where ω_g denotes the lowest natural circular frequency of the surface layer and h_g the corresponding critical damping ratio. Particularly, in the range of $\omega/\omega_g < 1$, the real part of K_r was approximated by

$$\text{Real part of } K_r = k_{rs} - I_s \omega^2$$

where k_{rs} means the spring constant of rotation due to the side reaction and I_s means the effective moment of inertia of soil. In a similar manner, the forcing moment M_f due to excitation of the stratum was given by

$$M_f = \frac{16aH^3 \rho}{\pi^2} \Gamma_1 (g_1 + ig_2) u_g \omega^2 e^{i\omega t}$$

where $-u_g \omega^2 e^{i\omega t}$ means the sinusoidal acceleration of the bed rock, ρ denotes the mass density of soil and the complex function $g_1 + ig_2$ is a nondimensional frequency response function alike to that a one-mass system of the natural frequency ω_g , though the apparent value of damping is somewhat larger than h_g .

Considering the above behaviours, the earthquake response of a building supported on a rigid underground structure embedded in a surface layer was dealt with. Furthermore, the theory was extended to treat of a flexible body alike to a pier. As an example, measured data of the earthquake response of a nuclear containment building, which is appropriate for the application of the present theory, are introduced and discussed.

Dynamic Analysis of a Structure Embedded
in an Elastic Stratum

by Hiroshi Tajimi

Synopsis

This paper deals with dynamic properties of a structure partially embedded in an elastic stratum and vertically supported on the underlying bed rock. It includes the spring constant, effective mass and radiation damping related to the lateral resistance of surrounding soil, and furthermore, input earthquake to the structure through the side wall in contact with soil. The analysis was performed by application of the three-dimensional wave propagation theory to the stratum overlying the bed rock. Besides, actual earthquake responses of a system appropriate to check the validity of the theory are illustrated.

1. Introduction

When a building is supported on a deep foundation, the earthquake response of the building is considerably affected by the surface layer (1). The reasons are that on the one hand the surface layer serves as a resistant medium against lateral movement of the structure, and on the other hand the distribution of underground acceleration usually becomes larger in the surface layer, as the depth are shallower. This paper describes a theoretical analysis of such structural response and field data obtained during natural earthquakes. In the analysis, the following assumptions were made:

- (1) The model ground consists of an elastic stratum resting on the bed rock.
- (2) A foundation structure of cylindrical shape, whose bottom rests on the bed rock, is embedded partially into the stratum.
- (3) The input acceleration, \ddot{u}_g , is applied on the surface of the bed rock.
- (4) The viscous damping of the stratum is taken into account for the shear wave traveling along the depth, though the damping is related principally to the impedance ratio between the surface layer and the underlying layer.
- (5) The vertical displacement of the surface layer is neglected, because it will be less significant than the other horizontal components.

Professor of Building Structure, Nihon University, Tokyo, Japan

2. Fundamental Equations

Let the cylindrical coordinates (r, θ, z) be set on the elastic layer under consideration, as shown in Fig. 1. If the wave equation for a homogeneous isotropic elastic medium may be applied to the concerned layer with a depth H , the equation can be written in the form

$$\begin{aligned} & (\lambda + 2\mu) \frac{\partial}{\partial r} \left[\frac{1}{r} \frac{\partial}{\partial r} (r u_r) + \frac{1}{r} \frac{\partial u_\theta}{\partial \theta} \right] - \mu \frac{1}{r} \frac{\partial}{\partial \theta} \left[\frac{1}{r} \frac{\partial}{\partial r} (r u_\theta) - \frac{1}{r} \frac{\partial u_r}{\partial \theta} \right] \\ & = \left(\rho \frac{\partial^2}{\partial t^2} - \mu \frac{\partial^2}{\partial z^2} - \mu' \frac{\partial^3}{\partial t \partial z^2} \right) u_r - \rho u_\theta \cos \theta \omega^2 e^{i\omega t} \end{aligned} \quad (1)$$

$$\begin{aligned} & (\lambda + 2\mu) \frac{1}{r} \frac{\partial}{\partial \theta} \left[\frac{1}{r} \frac{\partial}{\partial r} (r u_r) + \frac{1}{r} \frac{\partial u_\theta}{\partial \theta} \right] + \mu \frac{\partial}{\partial r} \left[\frac{1}{r} \frac{\partial}{\partial r} (r u_\theta) - \frac{1}{r} \frac{\partial u_r}{\partial \theta} \right] \\ & = \left(\rho \frac{\partial^2}{\partial t^2} - \mu \frac{\partial^2}{\partial z^2} - \mu' \frac{\partial^3}{\partial t \partial z^2} \right) u_\theta + \rho u_r \sin \theta \omega^2 e^{i\omega t} \end{aligned}$$

where u_r : horizontal displacement in the radial direction, relative to the bed rock,
 u_θ : horizontal displacement in the tangential direction, relative to the bed rock,
 λ, μ : Lamé's constants, ρ : mass density of soil.

General solutions of Eq. 1 are given by both general solutions for the homogeneous equations of Eq. 1, denoted by $(u_{r1}, u_{\theta 1})$, and the particular solutions denoted by $(u_{r2}, u_{\theta 2})$. In order to obtain the solution $(u_{r1}, u_{\theta 1})$, it is convenient to introduce the potential functions Q and S , which are defined by

$$\begin{aligned} u_{r1} &= \frac{\partial Q}{\partial r} + \frac{1}{r} \frac{\partial S}{\partial \theta} \\ u_{\theta 1} &= \frac{1}{r} \frac{\partial Q}{\partial \theta} - \frac{\partial S}{\partial r} \end{aligned} \quad (2)$$

Substituting Eq. 2 into the homogeneous equations of Eq. 1, one obtains

$$\begin{aligned} (\lambda + 2\mu) \nabla^2 Q &= \left(\rho \frac{\partial^2}{\partial t^2} - \mu \frac{\partial^2}{\partial z^2} - \mu' \frac{\partial^3}{\partial t \partial z^2} \right) Q \\ \mu \nabla^2 S &= \left(\rho \frac{\partial^2}{\partial t^2} - \mu \frac{\partial^2}{\partial z^2} - \mu' \frac{\partial^3}{\partial t \partial z^2} \right) S \end{aligned} \quad (3)$$

where

$$\nabla^2 = \frac{\partial^2}{\partial r^2} + \frac{1}{r} \frac{\partial}{\partial r} + \frac{1}{r^2} \frac{\partial^2}{\partial \theta^2}$$

To solve the above equations, one puts

$$\begin{aligned} Q &= \sum_{n=1,3,\dots}^{\infty} Q_n(r) \cos \theta \sin \frac{n\pi z}{2H} e^{i\omega t} \\ S &= \sum_{n=1,3,\dots}^{\infty} S_n(r) \sin \theta \sin \frac{n\pi z}{2H} e^{i\omega t} \end{aligned} \quad (4)$$

These expressions of Q and S satisfy the boundary condition that the shear stresses vanish at the free surface $z = H$. For successive calculations, it is convenient to define the following notations:

$$\frac{\lambda+2\mu}{\rho} = C_L^2, \quad \frac{\mu}{\rho} = C_T^2, \quad \frac{\mu+i\mu'\omega}{\rho} = C_T^2(1+i\frac{\mu'}{\mu}\omega)$$

$$C_T \frac{\pi}{2H} = \omega_g, \quad \sqrt{n^2(1+i\frac{\mu'}{\mu}\omega) - (\frac{\omega}{\omega_g})^2} = \xi_n, \quad \frac{\mu'}{\mu} = \frac{2h_g}{\omega_g}$$

where C_L and C_T are propagation velocities of longitudinal and transverse waves, respectively. The notation of ω_g denotes the lowest natural circular frequency of the surface layer given by

$$\omega_g = (\pi/2H) \sqrt{\mu/\rho}$$

and h_g denotes the corresponding critical damping ratio. Substitution of Eq. 4 into Eq. 3 yields

$$\begin{aligned} \left(\frac{d^2}{dr^2} + \frac{1}{r} \frac{d}{dr} - \left(\frac{\xi_n^2 \omega_g^2}{C_L^2} + \frac{1}{r^2} \right) \right) Q_n &= 0 \\ \left(\frac{d^2}{dr^2} + \frac{1}{r} \frac{d}{dr} - \left(\frac{\xi_n^2 \omega_g^2}{C_T^2} + \frac{1}{r^2} \right) \right) S_n &= 0 \end{aligned} \quad (5)$$

These equations are known to be satisfied by the modified Bessel functions:

$$\begin{aligned} Q_n &= A_n K_1 \left(\frac{\xi_n \omega_g r}{C_L} \right) \\ S_n &= B_n K_1 \left(\frac{\xi_n \omega_g r}{C_T} \right) \end{aligned} \quad (6)$$

where A_n and B_n are arbitrary constants. It follows that the potential functions are given by

$$\begin{aligned} Q &= \sum_{n=1,3,\dots}^{\infty} A_n K_1 \left(\frac{\xi_n \omega_g r}{C_L} \right) \cos \theta \sin \frac{n\pi z}{2H} e^{i\omega t} \\ S &= \sum_{n=1,3,\dots}^{\infty} B_n K_1 \left(\frac{\xi_n \omega_g r}{C_T} \right) \sin \theta \sin \frac{n\pi z}{2H} e^{i\omega t} \end{aligned} \quad (7)$$

Next, the particular solutions of Eq. 1 are obtained from solving the following equations:

$$\begin{aligned} \left(\rho \frac{\partial^2}{\partial t^2} - \mu \frac{\partial^2}{\partial z^2} - \mu' \frac{\partial^3}{\partial t \partial z^2} \right) u_r - \rho u_g \cos \theta \omega^2 e^{i\omega t} &= 0 \\ \left(\rho \frac{\partial^2}{\partial t^2} - \mu \frac{\partial^2}{\partial z^2} - \mu' \frac{\partial^3}{\partial t \partial z^2} \right) u_{\theta} + \rho u_g \sin \theta \omega^2 e^{i\omega t} &= 0 \end{aligned} \quad (8)$$

It results

$$\begin{aligned} u_{r2} &= u_g \left(\frac{\omega}{\omega_g} \right)^2 \cos \theta e^{i\omega t} \sum_{n=1,3,\dots}^{\infty} \frac{4}{n\pi} \frac{1}{\xi_n^2} \sin \frac{n\pi z}{2H} \\ u_{\theta 2} &= u_g \left(\frac{\omega}{\omega_g} \right)^2 \sin \theta e^{i\omega t} \sum_{n=1,3,\dots}^{\infty} \frac{4}{n\pi} \frac{1}{\xi_n^2} \sin \frac{n\pi z}{2H} \end{aligned} \quad (9)$$

Using these solutions, the displacements are given by

$$\begin{aligned} u_r &= \frac{\partial Q}{\partial r} + \frac{1}{r} \frac{\partial S}{\partial \theta} + u_{r2} \\ &= \sum_{n=1,3,\dots}^{\infty} \left\{ -A_n \left[\frac{1}{r} K_1 \left(\frac{\xi_n \omega_g r}{C_L} \right) + \frac{\xi_n \omega_g}{C_L} K_0 \left(\frac{\xi_n \omega_g r}{C_L} \right) \right] + \frac{B_n}{r} K_1 \left(\frac{\xi_n \omega_g r}{C_T} \right) \right. \\ &\quad \left. + \frac{4}{n\pi} \frac{u_g}{\xi_n^2} \left(\frac{\omega}{\omega_g} \right)^2 \right\} \cos \theta \sin \frac{n\pi z}{2H} e^{i\omega t} \end{aligned} \quad (10)$$

$$\begin{aligned}
u_\theta &= \frac{1}{r} \frac{\partial Q}{\partial \theta} - \frac{\partial S}{\partial r} + u_{\theta 2} \\
&= \sum_{n=1,3,\dots}^{\infty} \left\{ \frac{A_n}{r} K_1 \left(\frac{\xi_n \omega_g r}{C_L} \right) + B_n \left[\frac{1}{r} K_1 \left(\frac{\xi_n \omega_g r}{C_T} \right) + \frac{\xi_n \omega_g}{C_T} K_0 \left(\frac{\xi_n \omega_g r}{C_T} \right) \right] \right. \\
&\quad \left. - \frac{4}{n\pi} \frac{u_g}{\xi_n^2} \left(\frac{\omega}{\omega_g} \right)^2 \right\} \sin \theta \sin \frac{n\pi z}{2H} e^{i\omega t}
\end{aligned} \tag{11}$$

These expressions of displacements show that, as r approaches to infinity, the term involving the modified Bessel function tend zero, while the particular solutions are independent of r . It comes from that the particular solutions give the frequency response function of the elastic layer itself, so that it is not affected by existence of the rigid body. The displacement in the x -direction derived from the particular solutions can be written as

$$u_x = u_g \left(\frac{\omega}{\omega_g} \right) e^{i\omega t} \sum_{n=1,3,\dots}^{\infty} \frac{4}{n\pi} \frac{1}{n^2 - \left(\frac{\omega}{\omega_g} \right)^2 + i 2h_g \frac{\omega}{\omega_g}} \sin \frac{n\pi z}{2H} \tag{12}$$

From Eq. 12, the amplification factor $|(u_x + u_g)/u_g|$ at the surface $z = H$ in the resonant state $\omega = \omega_g$ is approximately written as

$$\left| \frac{u_x + u_g}{u_g} \right|_{\omega=\omega_g} \approx \frac{4}{\pi} \frac{1}{2h_g}$$

In the similar way, the general forms of stresses are given by

$$\begin{aligned}
\sigma_r &= \lambda \left(\frac{1}{r} \frac{\partial}{\partial r} (r u_r) + \frac{1}{r} \frac{\partial u_\theta}{\partial \theta} \right) + 2\mu \frac{\partial u_r}{\partial r} \\
&= \lambda r^2 Q + 2\mu \frac{\partial^2 Q}{\partial r^2} + 2\mu \left(\frac{1}{r} \frac{\partial^2 S}{\partial r \partial \theta} - \frac{1}{r^2} \frac{\partial S}{\partial \theta} \right) \\
&= (\lambda + 2\mu) r^2 Q + 2\mu \left(-\frac{1}{r} \frac{\partial Q}{\partial r} - \frac{1}{r^2} \frac{\partial^2 Q}{\partial \theta^2} + \frac{1}{r} \frac{\partial^2 S}{\partial r \partial \theta} - \frac{1}{r^2} \frac{\partial S}{\partial \theta} \right) \\
&= \sum_{n=1,3,\dots}^{\infty} \left\{ A_n \rho \xi_n^2 \omega_g^2 K_1 \left(\frac{\xi_n \omega_g r}{C_L} \right) + 2\mu A_n \left[\frac{2}{r^2} K_1 \left(\frac{\xi_n \omega_g r}{C_L} \right) + \frac{\xi_n \omega_g}{C_L r} K_0 \left(\frac{\xi_n \omega_g r}{C_L} \right) \right] \right. \\
&\quad \left. - 2\mu B_n \left[\frac{2}{r^2} K_1 \left(\frac{\xi_n \omega_g r}{C_T} \right) + \frac{\xi_n \omega_g}{C_T r} K_0 \left(\frac{\xi_n \omega_g r}{C_T} \right) \right] \right\} \cos \theta \sin \frac{n\pi z}{2H} e^{i\omega t}
\end{aligned} \tag{13}$$

$$\begin{aligned}
\tau_{r\theta} &= \mu \left(\frac{\partial u_\theta}{\partial r} - \frac{u_\theta}{r} + \frac{1}{r} \frac{\partial u_r}{\partial \theta} \right) \\
&= \mu \left(\frac{2}{r} \frac{\partial^2 Q}{\partial r \partial \theta} - \frac{1}{r^2} \frac{\partial Q}{\partial \theta} - 2 \frac{\partial^2 S}{\partial r^2} + r^2 S \right) \\
&= \mu r^2 S + 2\mu \left(\frac{1}{r} \frac{\partial^2 Q}{\partial r \partial \theta} - \frac{1}{r^2} \frac{\partial Q}{\partial \theta} + \frac{1}{r} \frac{\partial S}{\partial r} + \frac{1}{r^2} \frac{\partial^2 S}{\partial \theta^2} - r^2 S \right) \\
&= \sum_{n=1,3,\dots}^{\infty} \left\{ -B_n \rho \xi_n^2 \omega_g^2 K_1 \left(\frac{\xi_n \omega_g r}{C_T} \right) + 2\mu A_n \left[\frac{2}{r^2} K_1 \left(\frac{\xi_n \omega_g r}{C_L} \right) + \frac{\xi_n \omega_g}{C_L r} K_0 \left(\frac{\xi_n \omega_g r}{C_L} \right) \right] \right. \\
&\quad \left. - 2\mu B_n \left[\frac{2}{r^2} K_1 \left(\frac{\xi_n \omega_g r}{C_T} \right) + \frac{\xi_n \omega_g}{C_T r} K_0 \left(\frac{\xi_n \omega_g r}{C_T} \right) \right] \right\} \sin \theta \sin \frac{n\pi z}{2H} e^{i\omega t}
\end{aligned} \tag{14}$$

3. Rocking Motion of a Cylindrical Rigid Body Embedded in the Elastic Layer

To derive the equation of rocking motion of a rigid body, it must start to evaluate the reactive moment due to surrounding soil acting on the side surface of the rigid body. Assuming that the bottom surface of the rigid body has no sliding against the bed rock and furthermore the rocking axis coincides with a diameter of the bottom area, the reactive moment with respect to the rocking axis can be written in the form

$$\begin{aligned}
 M &= \int_0^H \left(\int_0^{2\pi} (\sigma_r|_{r=a} \cos \theta - \tau_{r\theta}|_{r=a} \sin \theta) a \, d\theta \right) z \, dz \\
 &= \sum_{n=1,3,\dots}^{\infty} \pi a \left(\frac{2H}{n\pi} \right)^2 (-1)^{\frac{n-1}{2}} [(\lambda+2\mu) \Delta Q_n + \mu \Delta S_n]_{r=a} \\
 &= \sum_{n=1,3,\dots}^{\infty} \rho \pi a \left(\frac{2H}{n\pi} \right)^2 (-1)^{\frac{n-1}{2}} \xi_n^2 \omega_g^2 \left[A_n K_1 \left(\frac{\xi_n \omega_g a}{C_L} \right) + B_n K_1 \left(\frac{\xi_n \omega_g a}{C_T} \right) \right] e^{i\omega t} \quad (15)
 \end{aligned}$$

where

$$\Delta = \frac{d^2}{dr^2} + \frac{1}{r} \frac{d}{dr} - \frac{1}{r^2}$$

The integral constants A_n and B_n are determined from the continuity conditions of displacements between soil and rigid body. If the rocking motion is given by a sinusoidal angular displacement $\varphi_0 e^{i\omega t}$, the continuity conditions of displacements can be expressed as

$$\begin{aligned}
 u_r|_{r=a} &= \varphi_0 z \cos \theta e^{i\omega t} = \frac{8\varphi_0 H}{\pi^2} \cos \theta \sum_{n=1,3,\dots}^{\infty} \frac{(-1)^{\frac{n-1}{2}}}{n^2} \sin \frac{n\pi z}{2H} e^{i\omega t} \\
 u_\theta|_{r=a} &= \varphi_0 z \sin \theta e^{i\omega t} = -\frac{8\varphi_0 H}{\pi^2} \sin \theta \sum_{n=1,3,\dots}^{\infty} \frac{(-1)^{\frac{n-1}{2}}}{n^2} \sin \frac{n\pi z}{2H} e^{i\omega t} \quad (16)
 \end{aligned}$$

Substituting Eqs. 10 and 11 into Eq. 16, the constants A_n and B_n are determined as follows:

$$\begin{aligned}
 \frac{A_n}{a} &= -\frac{1}{x_n} \left[2K_1 \left(\frac{\xi_n \omega_g a}{C_T} \right) + \frac{\xi_n \omega_g a}{C_T} K_0 \left(\frac{\xi_n \omega_g a}{C_T} \right) \right] \left[\frac{8\varphi_0 H}{\pi^2} \frac{(-1)^{\frac{n-1}{2}}}{n^2} - \frac{4}{n\pi} \frac{u_g}{\xi_n^2} \left(\frac{\omega}{\omega_g} \right)^2 \right] \\
 \frac{B_n}{a} &= -\frac{1}{x_n} \left[2K_1 \left(\frac{\xi_n \omega_g a}{C_L} \right) + \frac{\xi_n \omega_g a}{C_L} K_0 \left(\frac{\xi_n \omega_g a}{C_L} \right) \right] \left[\frac{8\varphi_0 H}{\pi^2} \frac{(-1)^{\frac{n-1}{2}}}{n^2} - \frac{4}{n\pi} \frac{u_g}{\xi_n^2} \left(\frac{\omega}{\omega_g} \right)^2 \right] \quad (17)
 \end{aligned}$$

where

$$\begin{aligned}
 x_n &= \left(K_1 \left(\frac{\xi_n \omega_g a}{C_L} \right) + \frac{\xi_n \omega_g a}{C_L} K_0 \left(\frac{\xi_n \omega_g a}{C_L} \right) \right) \left(K_1 \left(\frac{\xi_n \omega_g a}{C_T} \right) + \frac{\xi_n \omega_g a}{C_T} K_0 \left(\frac{\xi_n \omega_g a}{C_T} \right) \right) \\
 &\quad - K_1 \left(\frac{\xi_n \omega_g a}{C_L} \right) K_1 \left(\frac{\xi_n \omega_g a}{C_T} \right) \quad (18)
 \end{aligned}$$

Thus the reactive moment by Eq. 15 is determined as

$$M = - \sum_{n=1,3,\dots}^{\infty} a^2 \rho \pi \left(\frac{2H}{n\pi} \right)^2 (-1)^{\frac{n-1}{2}} \Omega_n \left[\frac{8\varphi_0 H}{\pi^2} \frac{(-1)^{\frac{n-1}{2}}}{n^2} - \frac{4}{n\pi} \frac{u_g}{\xi_n^2} \left(\frac{\omega}{\omega_g} \right)^2 \right] e^{i\omega t} \quad (19)$$

where

$$\begin{aligned}
 \Omega_n &= \frac{1}{x_n} \left[4K_1 \left(\frac{\xi_n \omega_g a}{C_L} \right) K_1 \left(\frac{\xi_n \omega_g a}{C_T} \right) + \frac{\xi_n \omega_g a}{C_T} K_1 \left(\frac{\xi_n \omega_g a}{C_L} \right) K_0 \left(\frac{\xi_n \omega_g a}{C_T} \right) \right. \\
 &\quad \left. + \frac{\xi_n \omega_g a}{C_L} K_1 \left(\frac{\xi_n \omega_g a}{C_T} \right) K_0 \left(\frac{\xi_n \omega_g a}{C_L} \right) \right] \quad (20)
 \end{aligned}$$

The parameters involved in the above equations can be written as

$$\frac{\xi_n \omega_g a}{C_T} = \xi_n \frac{\pi a}{2 H} , \quad \frac{\xi_n \omega_g a}{C_L} = \xi_n \frac{\pi a}{2 H} \frac{C_T}{C_L}$$

It follows that Ω_n can be represented by the function of n , ω/ω_g , a/H and C_T/C_L .

The moment given by Eq. 19 can be resolved into $M = -M_R + M_F$, in which $-M_R$ is the reactive moment induced by a motion of the rigid body relative to the surface layer and M_F represents the forcing moment to be imposed on the rigid body due to an excitation of the surface layer. This resolution may be simply explained as follows. If assuming that the rigid body undergoes a rocking motion with the rotational angle $\varphi = \varphi_0 e^{i\omega t}$ and at the same time the surface layer vibrates with the angular displacement $\varphi_s e^{i\omega t}$, as shown in Fig. 2, the reactive moment acting the rigid body are evidently written in the form

$$-K_R(\varphi_0 - \varphi_s) e^{i\omega t}$$

where K_R : reactive spring constant of soil.

The term $(-K_R \varphi_0 e^{i\omega t})$ corresponds to the former reactive moment and another term $K_R \varphi_s e^{i\omega t}$ is reduced to the latter forcing moment. In the present case, these moments are given from Eq. 19 as follows:

$$M_R = K_R \varphi_0 e^{i\omega t} = \frac{8\mu H^2 a}{\pi} \Gamma_1 (f_1 + if_2) \varphi_0 e^{i\omega t} \quad (21)$$

$$\Gamma_1 = \frac{a}{H} \sum_{n=1,3,5,\dots}^{\infty} \frac{\Omega_{ns}}{n^2} , \quad \Omega_{ns} = \Omega_n |_{\omega=0}$$

$$f_1 + if_2 = \left(\sum_{n=1,3,\dots}^{\infty} \xi_n^2 \Omega_n / n^4 \right) / \left(\sum_{n=1,3,\dots}^{\infty} \Omega_{ns} / n^2 \right)$$

$$M_F = \frac{16aH^3 \rho}{\pi^2} \Gamma_1 (g_1 + ig_2) u_g \omega^2 e^{i\omega t} \quad (22)$$

$$g_1 + ig_2 = \left(\sum_{n=1,3,\dots}^{\infty} \Omega_n (-1)^{\frac{n-1}{2}} / n^3 \right) / \left(\sum_{n=1,3,\dots}^{\infty} \Omega_{ns} / n^2 \right)$$

The function Γ_1 is dimensionless function of H/a and Poisson's ratio, and is shown diagrammatically in Fig. 3, where the ratio C_T/C_L is employed in place of Poisson's ratio. The complex function $f_1 + if_2$ gives dynamic effects and varies with ω/ω_g , h_g , C_T/C_L and a/H , as shown in Fig. 4. As a general tendency, it may be said that the real part f_1 , which gives spring rigidity, decreases with an increase of ω in the range of $\omega/\omega_g < 1$ and tends to a constant dependent of a/H for $\omega/\omega_g > 1$. The imaginary part f_2 , which provides with the radiation damping, is not significant in the range of $\omega/\omega_g < 1$, but rapidly increases in proportion to an increase of ω for $\omega/\omega_g > 1$. In Eq. 22. $(-u_g \omega^2 e^{i\omega t})$ means the sinusoidal acceleration of the underlying bed rock. The complex function $g_1 + ig_2$ is a nondimensional frequency response function alike to that for a

one-mass system of the natural frequency ω_g , as shown in Fig. 5.

Using thus obtained moment $M = -M_r + M_f$, the equation of rocking motion of a rigid body is written as

$$I \ddot{\varphi} + c_{rb} \dot{\varphi} + k_{rb} \varphi + M_r = mH_s u_g \omega^2 e^{i\omega t} + M_f \quad (23)$$

where I : mass moment of inertia of the rigid body about the rocking axis lied in the bottom area,

k_{rb} : spring constant of rocking of the rigid body associated with its bottom area,

c_{rb} : coefficient of equivalent viscous damping related to k_{rb} ,

m : mass of the rigid body,

H_s : height of the center of gravity of the rigid body from the bottom surface.

4. Approximate Method for Engineering Purposes

For practical purposes, it is desired to rewrite the reactive moment given by Eqs. 21 and 22 in more simple forms. In addition, it is to be noted that actual reactive moments are generated perhaps smaller than the theoretical values, because of soil properties having no tensile resistance. Hence, a reduction coefficient η is considered for the theoretical moment in the following calculations.

At first, as regards M_r given by Eq. 21, the real part f_1 may be approximated as

$$f_1 = 1 - \sqrt{2} (\omega/\omega_g)^2, \quad \omega/\omega_g < 1 \quad (24)$$

so as to be identical with the curves of f_1 drawn in Fig. 4. Then,

$$\begin{aligned} \text{Real part of } M_r &= (k_{rs} - I_s \omega^2) \varphi_o e^{i\omega t} \\ k_{rs} &= \frac{8\mu H^2 a}{\pi} \Gamma_1 \eta, \quad I_s = \frac{32a^2 H^3 \rho}{\pi^3} \frac{H}{a} \Gamma_1 \Gamma_2 \eta \end{aligned} \quad (25)$$

where k_{rs} means the spring constant of rotation due to the side reaction and I_s means the effective moment of inertia of soil. As a reference, the moment of inertia of the excluded soil by the body can be expressed as

$$I_a = \pi a^2 H^3 \rho \left[\frac{1}{4} \left(\frac{a}{H} \right)^2 + \frac{1}{3} \right]$$

The ratio I_s/I_a is plotted against H/a for the specific values of C_T/C_L and h_g in Fig. 6, when $\eta = 1$.

For M_f , Fig. 7 shows the resonance curves of $\sqrt{g_1^2 + g_2^2}$ versus ω/ω_g for the specific values of C_T/C_L , h_g and a/H . From these curves, one puts an approximate expression,

$$M_f = J_s F_s(\omega) u_g \omega^2 e^{i\omega t} \quad (26)$$

where

$$F_s(\omega) = \frac{1 + i2h_s(\omega/\omega_g)}{1 - (\omega/\omega_g)^2 + i2h_s(\omega/\omega_g)}, \quad J_s = \frac{16aH^3}{\pi^2} \Gamma_1 \eta \varepsilon_1|_{\omega=0}$$

Herein, the equivalent damping ratio h_s is plotted against h_g in Fig. 8. This indicates a linear relationship between h_s and h_g , almost independently of C_T/C_L and a/H .

The symbol J_s means the effective first moment of inertia of soil mass. Hence, denoting by J_a the first moment of the excluded soil mass about the rocking axis, that is $\pi a^2 H^2 \rho / 2$, the ratio J_s/J_a is given graphically in Fig. 9, when $\eta = 1$.

On the basis of thus obtained results, the equations of rocking motion of a shear building supported on a rigid underground structure (Fig. 10) are given by

$$\begin{aligned} m_i(x_i + H_i \ddot{\varphi}) + k_{i+1}(x_i - x_{i+1}) + k_i(x_i - x_{i-1}) &= -m_i \ddot{u}_g, \quad x_0 = 0 \\ m_i H_i(x_i + H_i \ddot{\varphi}) + (I_0 + I_s) \ddot{\varphi} + (k_{rb} + k_{rs}) \varphi &= -\sum_{i=0}^N m_i H_i \ddot{u}_g - J_s(\ddot{u} + \ddot{u}_g) \\ \ddot{u} + 2h_s \omega_g \dot{u} + \omega_g^2 u &= -\ddot{u}_g \end{aligned} \quad (27)$$

where I_0 : moment of inertia of the underground structure about the rocking axis,

k_{rb} : spring constant for rocking associated with the bottom area of the underground structure,

\ddot{u}_g : input earthquake acceleration at the bed rock.

In the above equations, the damping terms associated with the structure and structure-soil interaction are omitted, because of avoiding the confusion in the expressions.

5. Lateral Vibration of a Cylindrical Flexible Body Embedded in the Surface Layer

This problem is concerned in a pier foundation. For the theoretical analysis, the following assumptions were made:

- (1) A cylindrical elastic pier of radius a and of length H is supported on the bed rock, penetrating the overlying surface layer, as shown in Fig. 11.
- (2) The head of pier is fixed in the superstructure, which undergoes a horizontal translation.
- (3) The total shear force from the superstructure acts on the head of pier.

When $u_p(z, t)$ denotes the lateral displacement of the pier axis relative

to the bed rock, the equation of flexural vibration of the pier may be expressed in the form

$$\rho_p \pi a^2 \frac{\partial^2 u_p}{\partial t^2} + \ddot{u}_g + EI \frac{\partial^4 u_p}{\partial z^4} = (p(z) + q(z)) e^{i\omega t} \quad (28)$$

where ρ_p : equivalent mass density reduced to that for a solid pier with the diameter of a ,

EI : flexural stiffness of pier,

\ddot{u}_g : horizontal acceleration at the bed rock, $-u_g \omega^2 e^{i\omega t}$.

On the righthand side of Eq. 28, the function $p(z)e^{i\omega t}$ represents earth pressure acting on the circumference of the pier at the depth z in the x -direction. Using the similar way, with which Eq. 15 was derived, $p(z)$ can be written as

$$p(z) = \int_0^{2\pi} (\sigma_{r,\theta} \cos \theta - \tau_{r,\theta} \sin \theta) a d\theta$$

$$= \rho \pi a \sum_{n=1,3,\dots} \xi_n^2 \omega_g^2 \left[A_n K_1 \left(\frac{\xi_n \omega_g a}{C_L} \right) + B_n K_1 \left(\frac{\xi_n \omega_g a}{C_T} \right) \right] \sin \frac{n\pi z}{2H} \quad (29)$$

The second term $q(z)e^{i\omega t}$ represents the lateral force transmitted from the superstructure. If V denotes the concentrated shear force acting on the head of pier, one has

$$q(z) = \sum_{n=1,3,\dots}^{\infty} \frac{2V}{H} (-1)^{\frac{n-1}{2}} \sin \frac{n\pi z}{2H} \quad (30)$$

To solve Eq. 28, let the solution u_p be taken in the form of the Fourier series

$$u_p = \sum_{n=1,3,\dots}^{\infty} U_n \sin \frac{n\pi z}{2H} e^{i\omega t} \quad (30)$$

The integral constants A_n and B_n are determined by use of the continuity conditions of displacements between soil and pier:

$$u_p = u_r|_{r=a, \theta=0} = -u_\theta|_{r=a, \theta=\pi/2}$$

Thus, the solution of Eq. 28 is obtained as

$$u_p = \left[\frac{1}{EI} \left(\frac{2H}{\pi} \right)^4 \frac{2V}{H} F(z, \omega) + u_g G(z, \omega) \left(\frac{\omega}{\omega_g} \right)^2 \right] e^{i\omega t} \quad (31)$$

$$F(z, \omega) = \sum_{n=1,3,\dots}^{\infty} \frac{(-1)^{\frac{n-1}{2}}}{n^4 - \alpha_2 \frac{\rho_p}{\rho} \left(\frac{\omega}{\omega_g} \right)^2 + \alpha_2 \xi_n^2 \Omega_n} \sin \frac{n\pi z}{2H}$$

$$G(z, \omega) = \sum_{n=1,3,\dots}^{\infty} \frac{\alpha_2 \left(\Omega_n + \frac{\rho_p}{\rho} \right) \frac{4}{n\pi}}{n^4 - \alpha_2 \frac{\rho_p}{\rho} \left(\frac{\omega}{\omega_g} \right)^2 + \alpha_2 \xi_n^2 \Omega_n} \sin \frac{n\pi z}{2H}$$

where

$$\alpha_2 = \frac{\pi a^2}{EI} \left(\frac{2E}{\pi} \right)^2 \omega_g^2 = \frac{\pi}{EI} \left(\frac{2H}{\pi} \right)^4 \left(\frac{\pi a}{2H} \right)^2$$

The first term of Eq. 31 gives the displacement of the pier, the head of which is applied by the shear force $V e^{i\omega t}$. Hence, the ratio V/u_p for $\omega = 0$ and $z = H$ gives the statically horizontal spring constant of the pier-soil system:

$$k_h = \left[\frac{1}{EI} \left(\frac{2H}{\pi} \right)^4 \frac{2}{H} F(H, 0) \right]^{-1}$$

The second term gives the displacement of the pier, when the bed rock vibrates with the horizontal acceleration $-u_g \omega^2 e^{i\omega t}$ and the head is free from the external shear force.

On a numerical evaluation of Eq. 31, the calculation of $\alpha_2 \xi_n \Omega_n$ is very complicated. However, if $a \ll H$, a simplified method is useful, because the modified Bessel functions are approximated in the forms

$$K_0(\eta_{T_n}) = -\left(r + \log \frac{\eta_{T_n}}{2}\right), \quad K_1(\eta_{T_n}) = \frac{1}{\eta_{T_n}} + \left(r - 0.5 + \log \frac{\eta_{T_n}}{2}\right) \frac{\eta_{T_n}}{2}$$

$$K_0(\eta_{L_n}) = -\left(r + \log \frac{\eta_{L_n}}{2} + \log S\right), \quad K_1(\eta_{L_n}) = \frac{1}{\eta_{L_n} S} + \left(r - 0.5 + \log \frac{\eta_{L_n}}{2} + \log S\right) \times \frac{\eta_{L_n} S}{2}$$

where r : Euler's constant ($= 0.5772157\dots$), $s = C_T/C_L$,

$$\eta_{L_n} = \frac{\xi_n \omega_g a}{C_L} = \xi_n \frac{\pi a}{2H} \frac{C_T}{C_L}, \quad \eta_{T_n} = \frac{\xi_n \omega_g a}{C_T} = \xi_n \frac{\pi a}{2H}$$

Employing these approximation, one has

$$\alpha_2 \xi_n^2 \Omega_n = -\frac{4\mu\pi}{EI} \left(\frac{2H}{\pi} \right)^4 \frac{1}{(1+S^2) \left(r + \log \frac{\eta_{T_n}}{2} \right) + S^2 \log S} \quad (32)$$

As an example, consider a rigid structure supported by a pier foundation. Denoting by m the mass of the rigid structure per one pier and by $u_p(H)$ the relative displacement to the bed rock at the head of the pier, the shear force induced by the motion of the structure is given by

$$V e^{i\omega t} = -m \left[\ddot{u}_p(H) + \ddot{u}_g \right] = m\omega^2 \left[u_p(H) + u_g \right] e^{i\omega t} \quad (33)$$

Substituting Eq. 33 into Eq. 31, $u_p(H)$ can be determined. Then, it is convenient to define the natural frequency ω_B for the pier-soil system, obtained by use of the static spring constant:

$$\omega_B = \left[\frac{1}{EI} \left(\frac{2H}{\pi} \right)^4 \frac{2m}{H} F(H, 0) \right]^{-1/2} \quad (34)$$

The amplification of response of the rigid structure against the bed rock motion can be written as

$$\left| \frac{u_p(H) + u_g}{u_g} \right| = \left| \frac{1 + \left(\frac{\omega}{\omega_B} \right)^2 G(H, \omega)}{1 - \left(\frac{\omega}{\omega_B} \right)^2 \frac{F(H, \omega)}{F(H, 0)}} \right| \quad (35)$$

Fig. 12 shows a numerical example for the amplification of the pier, when $\mu I_0/EI = 10^{-3}$, $\rho_p/\rho = 1.6$, $\pi a/2H = 0.04$ and $C_T/C_L = 1/2$, where $I_0 = \pi a^4/4$.

From the figure, a feature is noticed that the peak at $\omega = \omega_g$ is rather higher than that at $\omega = \omega_s$. It means that in this case the surface layer has a significant effect on the behaviour of the pier.

6. Observatory Examples

(A) Earthquake response of a surface layer

Fig. 13 presents typical records of velocity measured in the boreholes at the selected depths. The soil profile in the vicinity of the site is indicated in Fig. 14, with the location of seismometers. As a general trend, it may be said that ground motions develop larger at shallower depths.

(B) Earthquake response of a composite system of surface layer and structure

The nuclear reactor containment building of the Japan Power Demonstration Reactor has been mounted by many seismometers to measure vibration of the structure as well as adjacent ground during natural earthquakes. The initial phase of observation has been reported at the Third World Conference on Earthquake Engineering.⁽²⁾ The containment building of a steel cylindrical shell is placed partly into the concrete caisson with the diameter of 20 m, and is supported on the concrete filled in the space between the shell and the caisson. The mat slab of the caisson rests on the sandy mud stone at a depth of 17.2 m below the ground surface.

Fig. 15 presents analog traces of typical accelerograms simultaneously recorded at the top of the caisson (+0.2 m G.L.) as well as the bottom of the surface layer (-17.2 m G.L.) in the same direction. In relation to the present theory, it is of interest to obtain the transfer function between at both places. For this purpose, plots of amplification factor versus frequency are drawn in Fig. 16 for different earthquakes. Herein, the amplification factor is defined by a ratio between response spectra of acceleration at the two places, evaluated with the critical damping ratio $h = 0.05$. It is obvious that there are two common peaks at the frequencies of about 3.0 and 4.5 cps. In particular, the peak for 4.5 cps was pronounced in most spectra, so that it was taken as the natural frequency of the concerned system. However, it has been proved later that the frequency of 4.5 cps is close to the dominant frequency of the surface layer, because the spectra at the bottom of the surface layer have a valley at 4.5 cps. It follows that another peak frequency of about 3.0 cps is assigned to that for the structure-soil system. This conversion seems to be supported by the numerical calculations based on the present theory, although the actual phenomenon are more complicated.

The coefficients of the forcing moments given by Eqs. 23 and 26 are obtained as

$$\begin{aligned} mH_s &= 1.33 \times 10^4 \text{ ton}\cdot\text{sec}^2 \\ J_s &= 1.95 \times 10^4 \text{ ton}\cdot\text{sec}^2 \\ I_s &= 1.057 \times 10^5 \text{ ton}\cdot\text{m}\cdot\text{sec}^2 \end{aligned}$$

using the basic data, $m = 1.29 \times 10^3 \text{ ton}\cdot\text{sec}^2/\text{m}$, $I = 2.416 \times 10^5 \text{ ton}\cdot\text{m}\cdot\text{sec}^2$, $H_s = 10.3 \text{ m}$, $a = 10 \text{ m}$, $H = 17 \text{ m}$, $\rho = 1.6/9.8 \text{ ton sec}^2/\text{m}^4$, $\bar{I}_1 = 3.0$ from Fig. 3, $\bar{I}_2 = 0.5$ as an approximation from Fig. 4 and $\eta = 0.5$ assumed.

Hence, it may be supposed that the forcing moment due to the action of the surface layer is considerably larger than that due to the mass inertia of the structure itself. To make it sure, the response at the top of the caisson, $x + u_g$, was computed by use of the following equations similar to Eq. 27:

$$\begin{aligned} \ddot{x} + 2h_o\omega_o\dot{x} + \omega_o^2x &= -\frac{mH_sH_o}{I + I_s}\ddot{u}_g - \frac{J_sH_o}{I + I_s}(\ddot{u} + \ddot{u}_g) \\ \ddot{u} + 2h_s\omega_g\dot{u} + \omega_g^2u &= -\ddot{u}_g \end{aligned} \quad (36)$$

where ω_o : natural frequency of the structure-soil system in the rocking mode,

h_o : equivalent critical damping ratio associated with the concerned rocking mode,

H_o : height of the top of the caisson above the bottom (= 17.2 m).

Comparisons of thus computed response with the observed one are illustrated in Fig. 15, where the selected values of ω_o , h_o , ω_g and h_s are indicated. For the coefficients of $mH_sH_o/(I + I_s)$ and $J_sH_o/(I + I_s)$, the theoretical values of 0.65 and 0.92 respectively were taken. By inspection of the figures, it is concluded that a rough agreement between the theoretical and observed response can be assured, in spite of a simplified approach.

References

- (1) Penzien, J., Scheffey, C., and Parmelee, R., "Seismic Analysis of Bridges on Long Piles," Journal of the Engineering Mechanics Division, ASCE, Vol. 90, No. EM3, Proc. Paper 3953, June, 1964, pp. 223-254.
- (2) Tajimi, H., Ohmura, M., Uchida, T., and Akino, K., "Observed Vibrations of a Nuclear Reactor Building During Some Weak Earthquakes," Proc. the 3rd W.C.E.E., 1965.

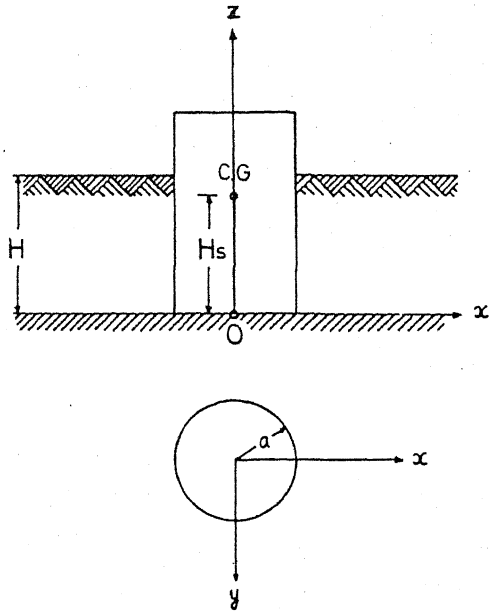


Fig. 1

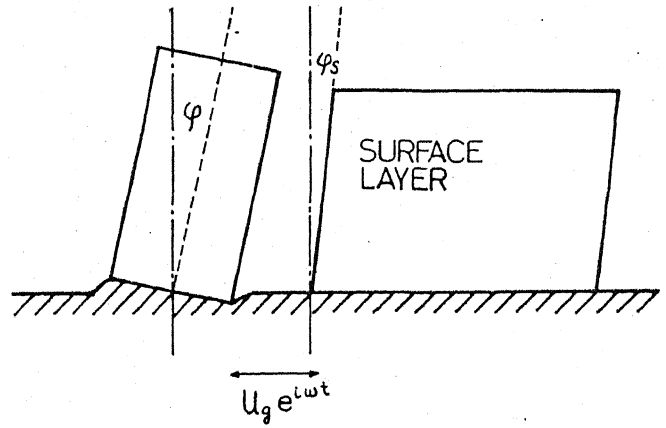


Fig. 2

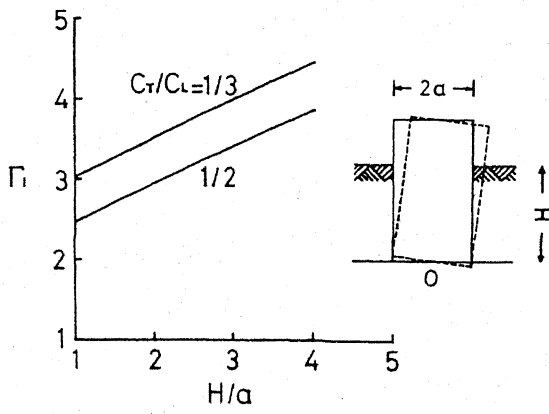


Fig. 3

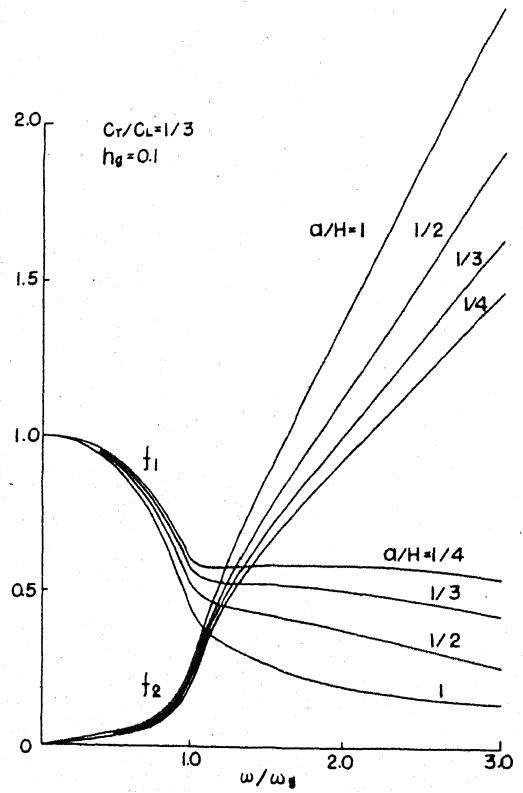


Fig. 4

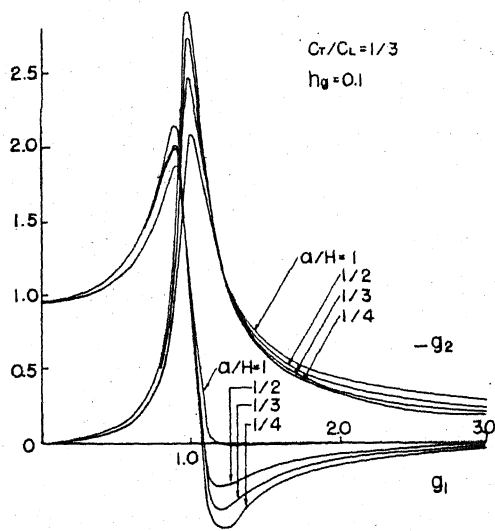


Fig. 5

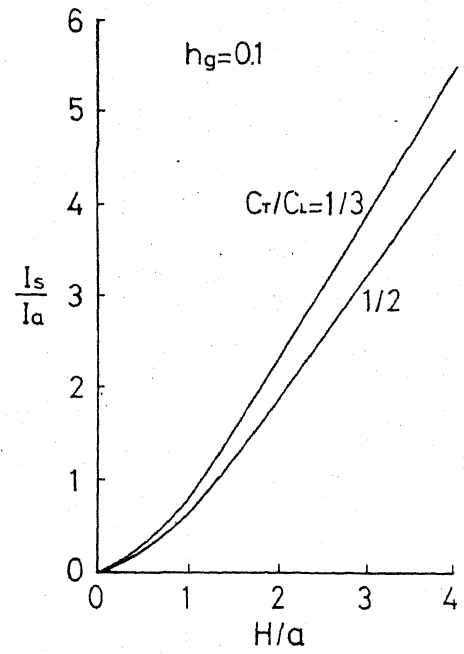


Fig. 6

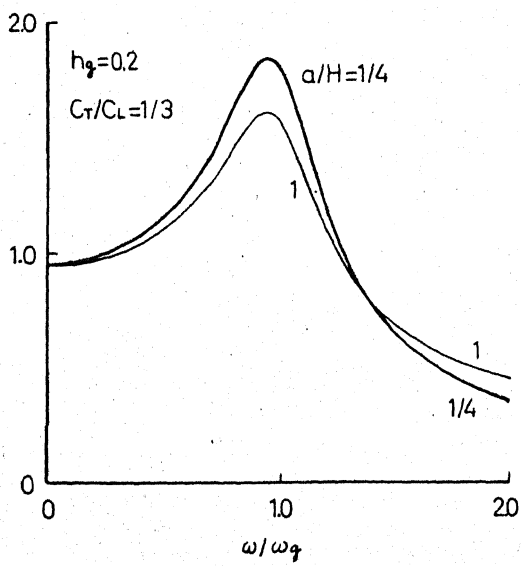


Fig. 7

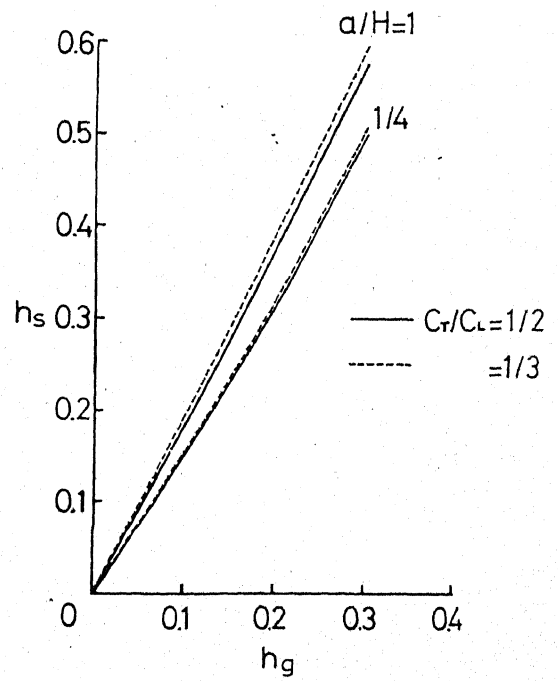


Fig. 8

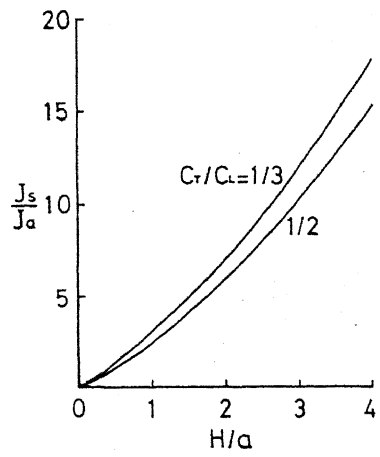


Fig. 9

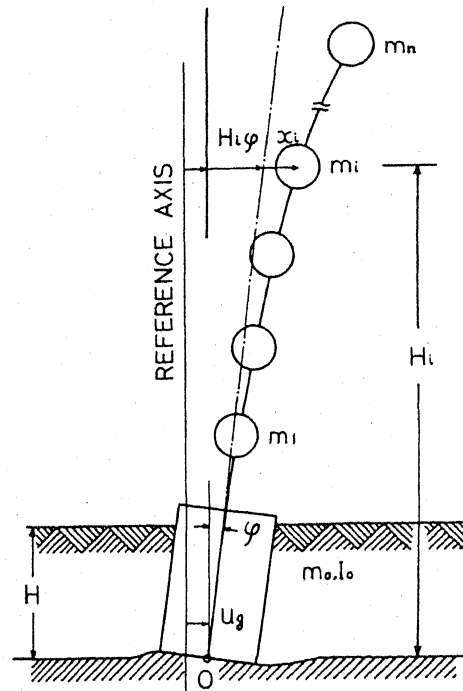


Fig. 10

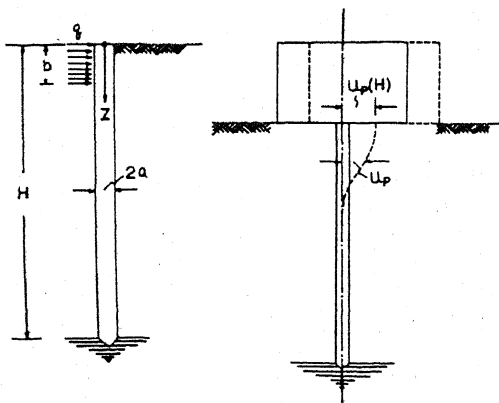


Fig. 11

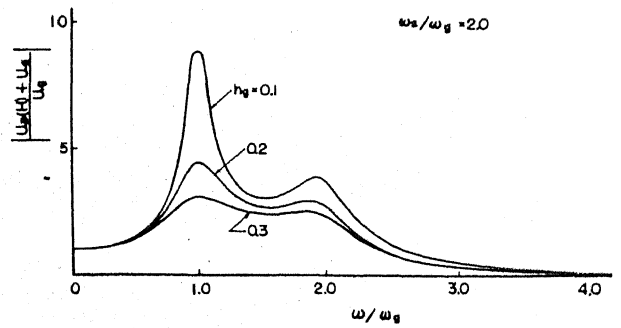


Fig. 12

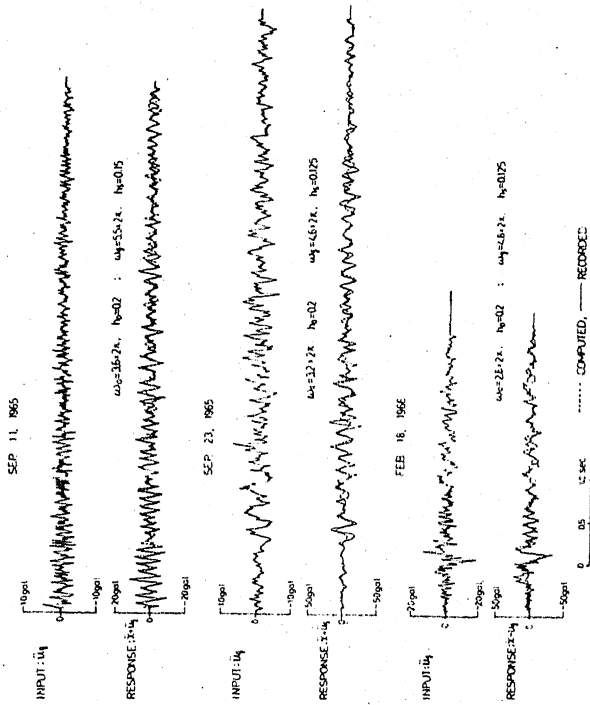


Fig. 15

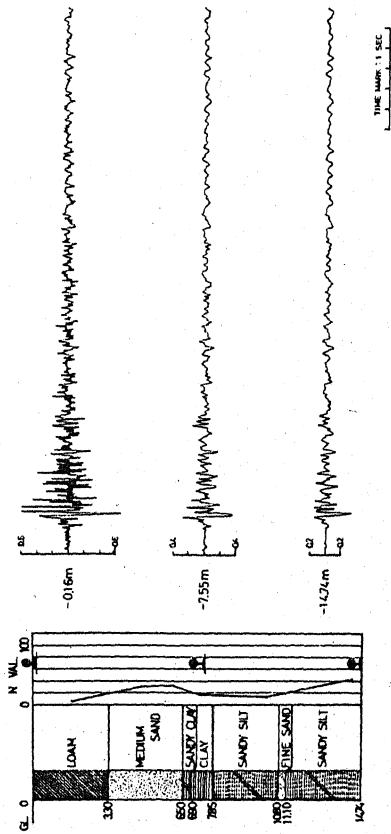


Fig. 14

Fig. 13

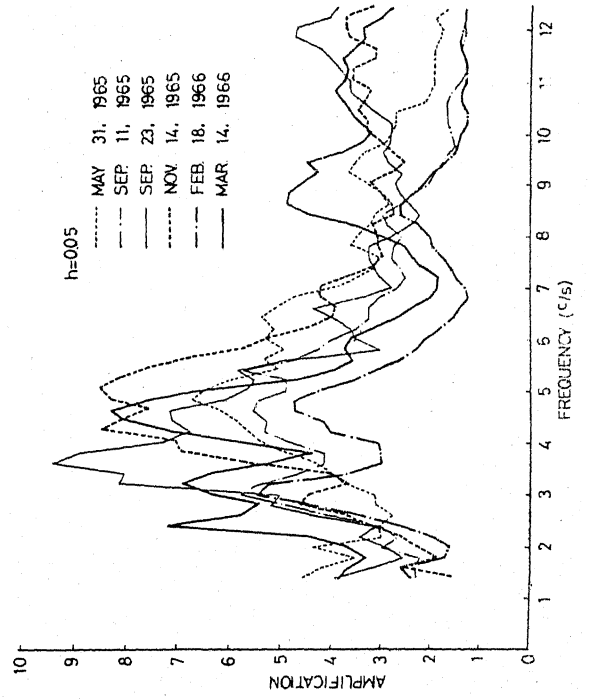


Fig. 16